

Synthesis and evaluation of a new water soluble corrosion inhibitor from recycled poly(ethylene terephthalate)

M.A. Migahed^{a,*}, A.M. Abdul-Raheim^a, A.M. Atta^a, W. Brostow^b

^a Egyptian Petroleum Research Institute, Petroleum Application, Ahmed Al Zomr St., Nasr City, Cairo 11727, Egypt

^b University of North Texas, USA

ARTICLE INFO

Article history:

Received 15 March 2009

Received in revised form

28 December 2009

Accepted 8 January 2010

Keywords:

Polyethylene terephthalate waste (PET)

Glycolized (GT)

Thiol derivative (GT-SH)

Corrosion inhibitor

API XL65 carbon steel

Electrochemical impedance spectroscopy

(EIS)

Energy dispersive X-ray analysis (EDX)

ABSTRACT

Polyethylene terephthalate waste (PET) was depolymerized by triethanolamine into glycolized product (GT), followed by esterification with bromoacetic acid in the presence of manganese acetate as a catalyst to give (GT-Br). The obtained ester was reacted with thiourea to give thiol derivative (GT-SH). The effectiveness of the synthesized compound as corrosion inhibitor for API XL65 carbon steel, in 2 M hydrochloric acid solution was investigated by various electrochemical techniques such as open circuit potential, potentiodynamic polarization and electrochemical impedance spectroscopy (EIS). The results of these investigations showed enhancement in inhibition efficiencies with the increasing of inhibitor concentration. The protective film formed on carbon steel surface was analyzed using an energy dispersive X-ray analysis (EDX) technique. Also, scanning electron microscope (SEM) was used to study the surface morphology of steel surface in the absence and presence of 400 ppm of the additive.

© 2010 Elsevier B.V. All rights reserved.

1. Introduction

Polyethylene terephthalate (PET) is a worldwide used polymer, and packaging is one of its most important applications. Due to its high resistance to the atmospheric and biological agents, this polymer is not considered as biodegradable. PET is not a hazardous product, but its waste quantity increases drastically and so it is a good candidate for recycling. PET waste can be recycled by different methods like physical recycling and chemical recycling. Chemical recycling is the reaction of PET with various reagents to obtain products that are used in the chemical industry [1].

Corrosion problem is one of the major concerns in the oil and gas industry. Therefore protection of metallic structures against corrosion regarded as a critical subject. Acid solutions were widely used in industrial acid cleaning, acid descaling, acid picking and oil-well acidizing. In these acid solutions corrosion inhibitors are required in order to restrain the acid erosion of metallic materials [2]. The adsorption of organic molecules at the metal/solution interface is of a great interest in surface science and can markedly change the corrosion resistance of the metal [3]. Most of the well-

known acid inhibitors are organic compounds containing nitrogen, sulfur and/or oxygen atoms [4–23].

In this work, we tried to modify the glycolized PET into thiol compound to be used as a corrosion inhibitor. Also, the work is devoted to study the inhibition characteristics of the environmental friendly synthesized additive for corrosion of API XL65-type carbon steel in 2 M HCl solution using both polarization and electrochemical impedance spectroscopy (EIS) techniques. The obtained data were confirmed by energy dispersive X-ray analysis (EDX) and scanning electron microscopy (SEM).

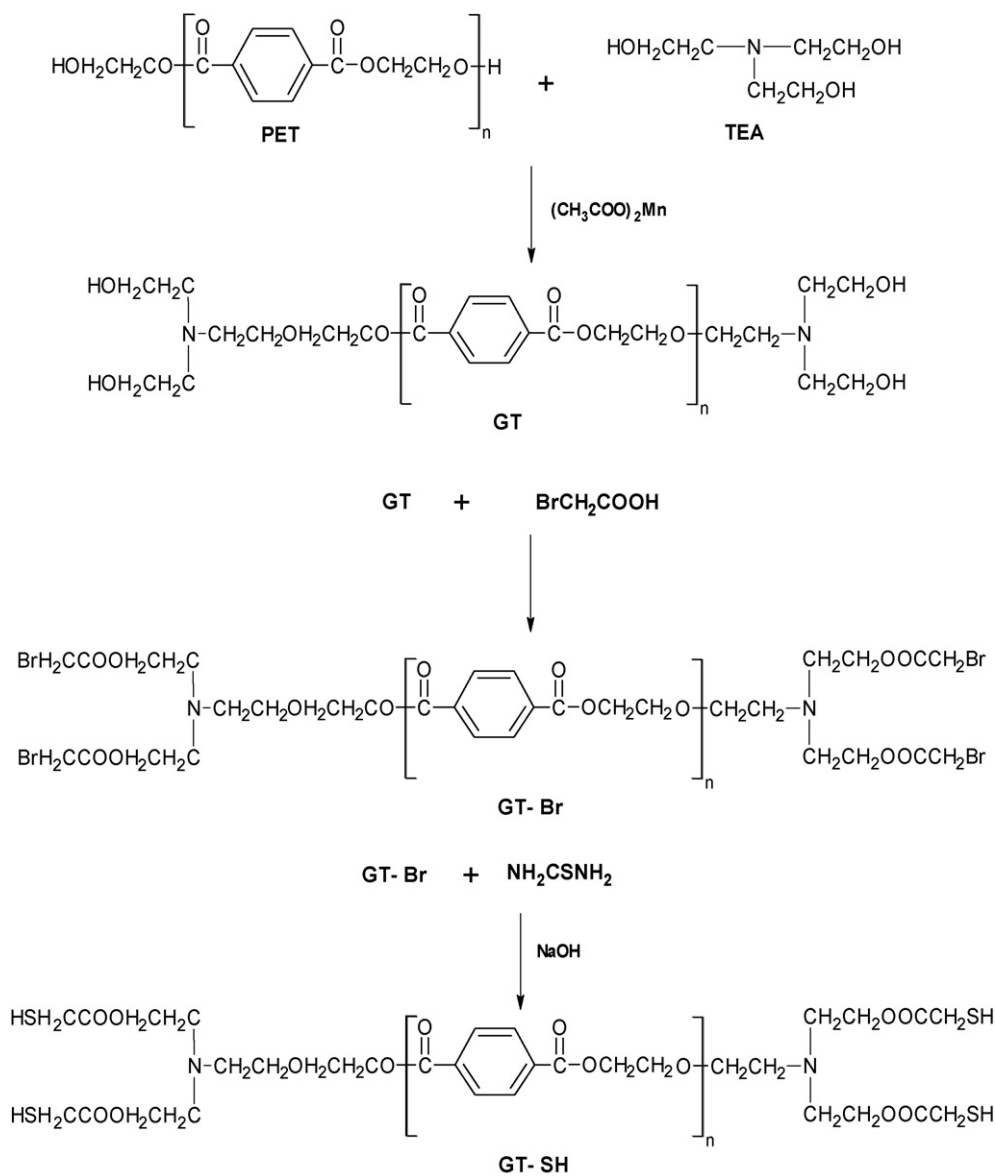
2. Experimental techniques

2.1. Synthesis and characterization of the inhibitor

PET bottle waste was depolymerized at weight ratio of PET to triethanolamine (TEA) 1:1 (wt% of PET: wt% of TEA) using 0.5% of manganese acetate as catalyst (by weight based on weight of PET). The reaction mixtures were heated under vigorous stirring in nitrogen atmosphere at temperature about 443–463 K for 4 h and at 473–483 K for 3 h. The temperature of the reaction was then lowered to 373 K for 1 h. The mixture was allowed to cool to room temperature. The glycolized product of PET with TEA is designated as GT. Free TEA was removed by dissolving the glycolized product in acetone and then precipitated by diethyl ether. The oligomers were filtered and the solvents were removed under reduced pressure. The difference between the initial and final weights represents the amount of free TEA. GT-bromoacetate (GT-Br) was prepared by esterification of 0.1 mol of GT and 0.4 mol of bromoacetic acid in the presence of 1% (by weight) of p-toluene sulfonic acid (PTSA). The reaction mixture was heated up to 120 °C to remove the theoretical condensed water using Dean–Stark separator. The product was precipitated in

* Corresponding author. Tel.: +20 106952123.

E-mail address: mohamedatiyya707@hotmail.com (M.A. Migahed).



diethyl ether and the obtained precipitate was filtered off and washed with diethyl ether. GT-Br was converted into thiol derivative (GT-SH) via the isothiouranium salt by reaction with thiourea [24]. GT-Br (0.1 mol) and thiourea (0.4 mol) were dissolved in deoxygenated ethanol (200 mL) and refluxed for 6 h. The reaction mixture was concentrated and the residue was washed with hexane and recrystallized from ethanol/hexane (yield 95%). This intermediate salt was dissolved in 150 mL of ethanol, and then an aqueous solution (5 mL) of NaOH (70 mg) was added drop wise. The mixture was refluxed for 2 h after neutralization with sulfuric acid and the reaction mixture was concentrated. The residue was dissolved in diethyl ether and dried over Na_2SO_4 . The solution was evaporated and the residue was dissolved in hot ethanol and filtered to remove undissolved by-products (sulfide or disulfide derivatives). Evaporation and crystallization from CHCl_3 /ethanol gave GT-SH. The method of synthesis is summarized in Scheme 1. The chemical structure of the GT oligomer and G-SH was confirmed from their IR spectra. The spectra of GT and GT-SH were represented in Fig. 1(a) and (b), respectively. The presence of strong band at 3450 cm^{-1} , in spectrum of GT indicates the termination of the glycolized (GT) product with hydroxyl groups and the band observed at 810 cm^{-1} for GT is assigned to $-\text{CH}$ out-of-plane bending of *p*-substituted phenyl. This confirms the presence of phenyl rings in depolymerized product (GT). The presence of strong bands at 1745 and 1150 cm^{-1} , which were assigned for $\text{C}=\text{O}$ stretching and $\text{C}-\text{O}$ stretching of ester groups, indicates the incorporation of ester groups in GT product (Fig. 1a). The appearance of new band at 2350 cm^{-1} , which represents SH stretching, in spectrum of GT-SH (Fig. 1b) indicates the formation of thiol derivative.

A further confirmation for formation of thiol derivative from GT was determined from ^1H NMR analysis. In this respect the spectra of GT and GT-SH were repre-

sented in Fig. 2(a) and (b), respectively. The signals at chemical shifts 8, 4.8 and 4.3 ppm, represent *p*-substituted phenyl group, $\text{OOCCH}_2\text{CH}_2\text{COO}$ and $\text{OCH}_2\text{CH}_2\text{N}$ of GT respectively, were observed in all spectra. The signal observed at 2.6 ppm in the spectra of GT, which represent OH group of glycolized GT, indicate the presence of terminal OH in GT derivative (Fig. 2a). The appearance of new signals at 2.5 and 4.3 ppm which represent CH_2S and SH protons, in spectrum of GT-SH (Fig. 2b) indicates the formation of thiol derivative.

2.2. Preparation of aggressive solution

The aggressive solution (2 M HCl) was prepared by appropriate dilution of analytical grade 37% HCl with double distilled water.

2.3. Surface preparation of carbon steel

API XL65-type carbon steel sheets (obtained from PETROJET Petroleum Company, Egypt) containing 0.16% C, 0.10% Si, 0.40% Mn, 0.02% S, 0.13% P, 0.004 Cr and the remainder Fe were used in this study. A carbon steel disc of the same chemical composition was mounted in Teflon with an exposed surface area of 1 cm^2 was used in all electrochemical measurements. The prepared electrode was mechanically polished with different grades of silicon carbide papers, degreased in ethanol to obtain a fresh oxide-free surface [25], washed with bi-distilled water and dried at room temperature.

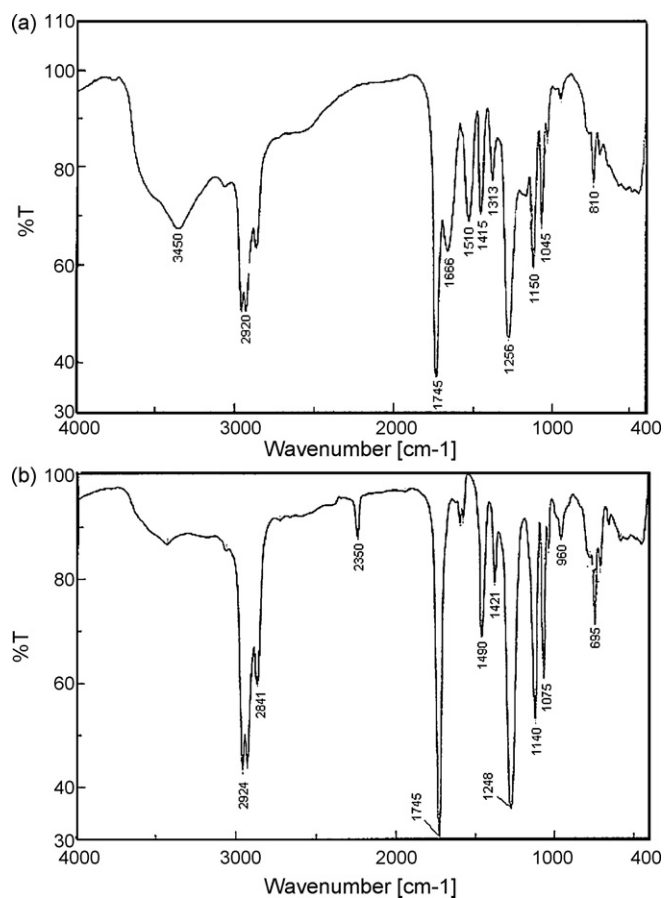


Fig. 1. FTIR spectra of (a) GT and (b) GT-SH.

2.4. Open circuit potential measurements

The potential of carbon steel electrodes was measured against the saturated calomel electrode (SCE) in 2 M HCl solution in the absence and presence of various inhibitor concentrations until the open circuit potential is reached.

2.5. Potentiodynamic polarization measurement

Potentiodynamic polarization studies were carried out using Volta lab 40 (Tacussel-Radiometer PGZ301) potentiostat and controlled by Tacussel corrosion analysis software model (Voltmaster 4) at a scan rate of 5 mV s^{-1} under static condition. A platinum electrode and saturated calomel electrodes (SCE) were used as auxiliary and reference electrodes, respectively. The working electrode was prepared from a cylindrical carbon steel rod insulated with polytetrafluoethylene tape (PTFE). The area exposed to the aggressive solution was 1 cm^2 . All the experiments were carried out at constant temperature of $30 \pm 1^\circ \text{C}$.

2.6. Electrochemical impedance measurement

AC impedance measurements were performed using Tacussel-Radiometer PGZ 301 Frequency Response Analyzer in a frequency range from 10^5 to 10^{-2} Hz with 10 points per decade. An AC sinusoid $\pm 10 \text{ mV}$ was applied at the corrosion potential (E_{corr}). The experiments were measured after 6 h of immersion. The impedance data were analyzed and fitted using graphing and analyzing impedance software, version Voltmaster 4.

2.7. Energy dispersive analysis of X-ray (EDX)

EDX system attached with a Joel 5400 scanning electron microscope was used for elemental analysis or chemical characterization of the film formed on steel surface. As a type of spectroscopy, it relies on the investigation of sample through interaction between electromagnetic radiation and the matter. So that, a detector was used to convert X-ray energy into voltage signals. This information is sent to a pulse processor, which measures the signals and passed them into an analyzer for data display and analysis.

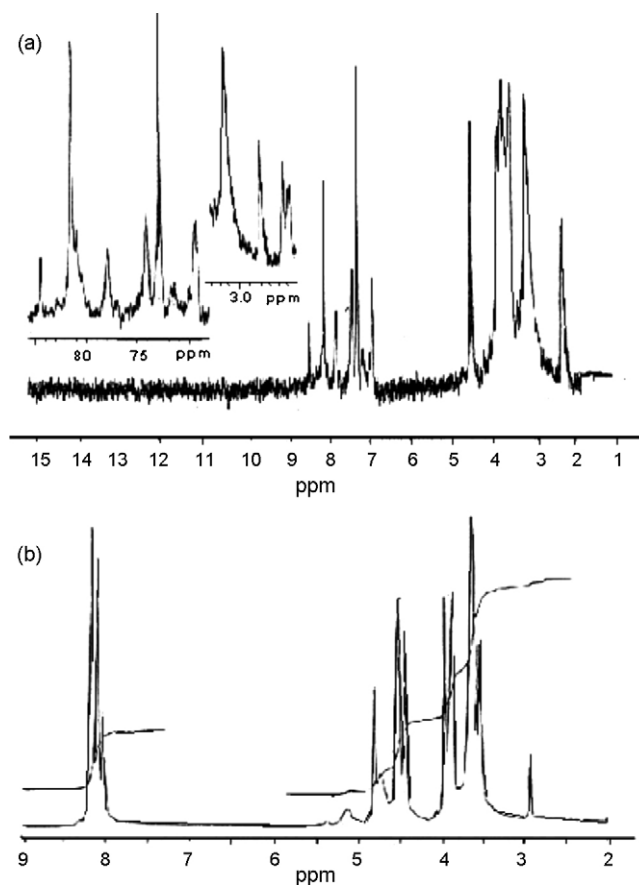


Fig. 2. NMR spectra of (a) GT and (b) GT-SH.

2.8. Scanning electron microscopy (SEM)

The surface examination was carried out using scanning electron microscope (Jeol 5400, Japan); the energy of the acceleration beam employed was 30 kV. All micrographs were carried out at a magnification power of $X = 1500$.

3. Results and discussion

3.1. Open circuit potential measurements

The potential of carbon steel electrodes immersed in 2 M HCl solution was measured as a function of immersion time in the absence and presence of 400 ppm of (GT-SH) as shown in Fig. 3. It is clear that the potential of carbon steel electrode immersed in 2 M HCl solution (blank curve) tends towards more negative potential firstly, giving rise to short step. This behavior was reported by

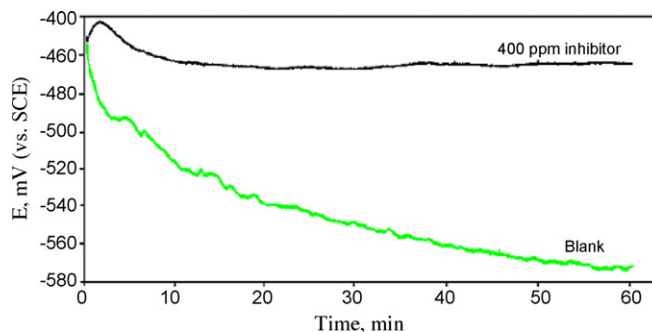


Fig. 3. Potential–time curves for carbon steel immersed in 2 M HCl solution in the absence and presence of 400 ppm of (GT-SH).

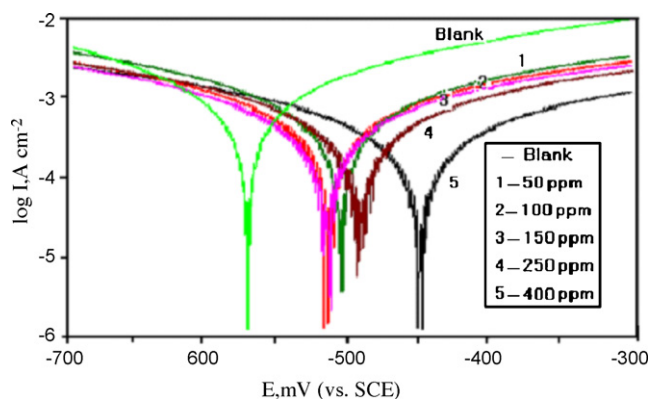


Fig. 4. Potentiodynamic polarization curves for carbon steel immersed in 2 M HCl solution in the absence and presence of various concentrations of (GT-SH).

West [26], which represents the break down of the pre-immersion air formed oxide film presents on the surface according to the following equation:



This is followed by the growth of a new oxide film inside the solution, so that the potential was shifted again to more noble direction until steady state potential is established. Addition of inhibitor molecules to the aggressive medium produces a negative shift in the open circuit potential due to the retardation of the cathodic reaction.

3.2. Potentiodynamic polarization measurements

The effect of inhibitor concentration on both anodic and cathodic curves of carbon steel in 2 M HCl solution was studied using potentiodynamic polarization technique. The obtained results are shown in Fig. 4. Also, the electrochemical parameters such as I_{corr} , E_{corr} , β_a and β_c and R_p associated with polarization measurements for carbon steel at different concentrations of the additive were simultaneously determined from the polarization curves using Voltmaster 4 corrosion software and are listed in Table 1. As reflected from the plots the additive exhibits a significant effect on the current–potential relations. The following points could also be withdrawn:

- The Tafel lines are shifted to more negative and more positive potentials for the cathodic and anodic process, respectively relative to the blank curve. This means that the additive affects both anodic dissolution of the metal and cathodic evolution of hydrogen (i.e. mixed-type inhibitor).
- The slopes of the cathodic and anodic Tafel lines are approximately constant and independent on the inhibitor concentration. This behavior suggests that the inhibitor molecules affect the corrosion rate of carbon steel without changing the metal dissolution mechanism [27].

Table 1

Data obtained from potentiodynamic polarization measurements of carbon steel immersed in 2 M HCl solution in the absence and presence of various concentrations of (GT-SH).

Concentration of the inhibitor (ppm)	E_{corr} , mV (vs. SCE)	I_{corr} ($\mu\text{A cm}^{-2}$)	β_c (mV dec $^{-1}$)	β_a (mV dec $^{-1}$)	R_p ($\text{k}\Omega \text{cm}^2$)	Coeff.	η (%)
2 M HCl (blank)	−568	316	134	95	0.07	0.98	–
50 ppm	−522	127	132	94	0.19	0.99	59.8
100 ppm	−506	82	127	93	0.28	0.99	74.1
150 ppm	−492	75	125	92	0.31	0.99	76.2
250 ppm	−478	61	122	91	0.37	0.98	80.6
400 ppm	−454	45	121	89	0.49	0.97	85.7

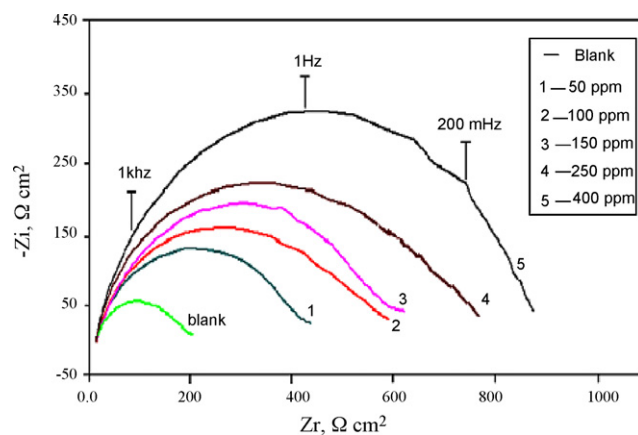


Fig. 5. Nyquist plots for carbon steel immersed in 2 M HCl solution in the absence and presence of various concentrations of (GT-SH).

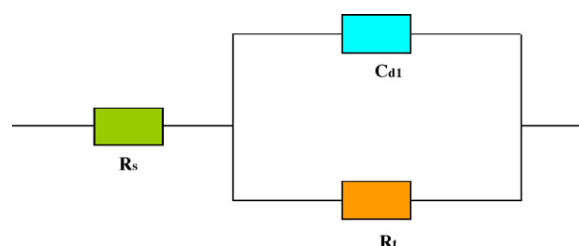


Fig. 6. The equivalent circuit model for the electrochemical impedance measurements.

- By increasing the concentration of the additive the corrosion current densities (I_{corr}) was decreased.

This behavior can be attributed to adsorption of the inhibitor molecules on carbon steel surface forming a protective layer [28]. The formation of such protective film was examined by EDX and SEM.

3.3. EIS measurements

Fig. 5 shows Nyquist plots recorded for carbon steel electrode immersed in 2 M hydrochloric acid solution at 30 ± 1 °C in the absence and presence of various concentrations of the inhibitor at the respective open circuit potentials. It is clear from the figure that imperfect semicircles were obtained. This behavior can be attributed to frequency dispersion [29]. For analysis of the impedance spectra containing one capacitive loop, a simple equivalent circuit consisting of a parallel combination of a capacitor, C_{dl} , and a resistor, R_t , in series with a resistor, R_s , representing the solution resistance. The proposed equivalent circuit is shown in Fig. 6. The electrode impedance, Z , in this case is represented by the

Table 2

Data from electrochemical impedance spectroscopy measurements of carbon steel in 2 M HCl solution in the absence and presence of various concentrations of (GT-SH).

Concentration of the inhibitor (ppm)	R_t ($\Omega \text{ cm}^2$)	C_{dl} ($\mu\text{F cm}^{-2}$)	α	η (%)
2 M HCl (blank)	178	147	0.93	-
50 ppm	426	61	0.94	55.7
100 ppm	605	44	0.95	72.3
150 ppm	644	39	0.96	79.7
250 ppm	775	33	0.98	86.2
400 ppm	938	24	0.98	87.1

mathematical formulation [30]:

$$Z = R_s + \left[\frac{R_t}{1 + (2\pi f R_t C_{dl})^\alpha} \right] \quad (2)$$

where α denotes an empirical parameter ($0 \leq \alpha \leq 1$) and f is the frequency in Hz. Eq. (2) takes into account the deviation from the ideal RC-behavior in terms of a distribution of time constant due to surface heterogeneity, roughness effects, adsorption of inhibitors and variations in properties or compositions of surface layers. Various electrochemical parameters derived from Nyquist plots are calculated and listed in Table 2.

The values of R_t were given by subtracting the high frequency impedance from the low frequency one as follows [31]:

$$R_t = Z'_{re.} (\text{at low frequency}) - Z'_{re.} (\text{at high frequency}) \quad (3)$$

The values of electrochemical double layer capacitance C_{dl} were calculated at the frequency f_{max} , at which the imaginary component of the impedance is maximal ($-Z_{max}$) by the following equation [32]:

$$C_{dl} = \frac{1}{2\pi f_{max}} \frac{1}{R_t} \quad (4)$$

The values of percentage inhibition efficiency (η , %) were calculated from the values of R_t according to the following equation [33]:

$$\eta, \% = \frac{R_{t(inh.)} - R_t}{R_{t(inh.)}} \quad (5)$$

where R_t and $R_{t(inh.)}$ are the values of the charge transfer resistance in the absence and presence of the inhibitor, respectively. The impedance data listed in Table 2 indicate that the values of both R_t and η , % are found to increase by increasing the inhibitor concentration, while the values of C_{dl} are found to decrease. This behavior can be attributed to a decrease in dielectric constant and/or an

increase in the thickness of the electrical double layer, suggesting that the inhibitor molecules act by adsorption mechanism at carbon steel/acid interface [34]. Bode plots are shown in Fig. 7. The plots indicate the presence of one time constant, corresponding to one depressed semicircle that obtained in case of Nyquist plots. For comparison, the variation of the values of percentage inhibition efficiency (η , %) with the inhibitor concentration obtained

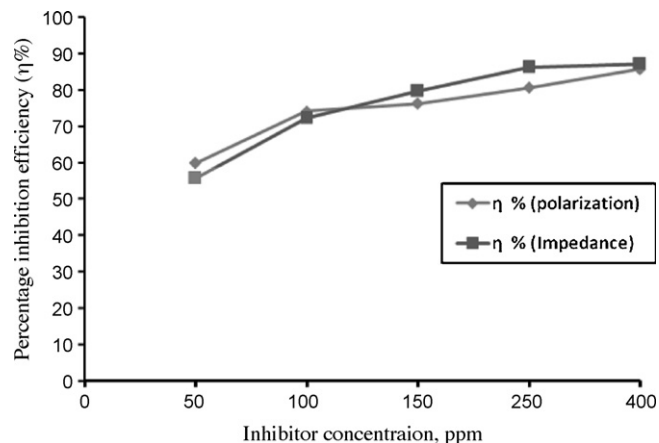


Fig. 8. Variation of the percentage inhibition efficiency (η , %) with the concentration of (GT-SH).

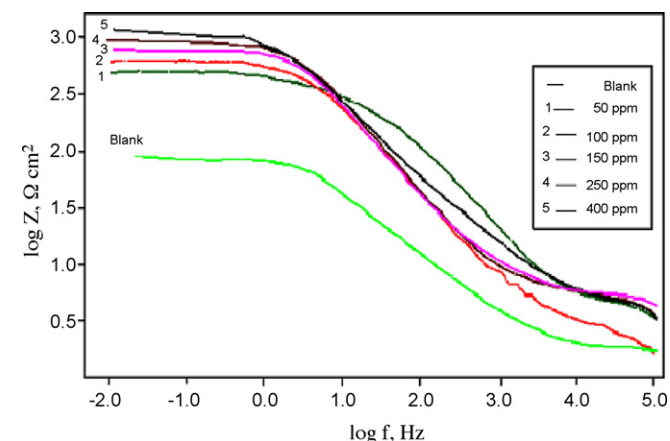


Fig. 7. Bode plots for carbon steel immersed in 2 M HCl solution in the absence and presence of various concentrations of (GT-SH).

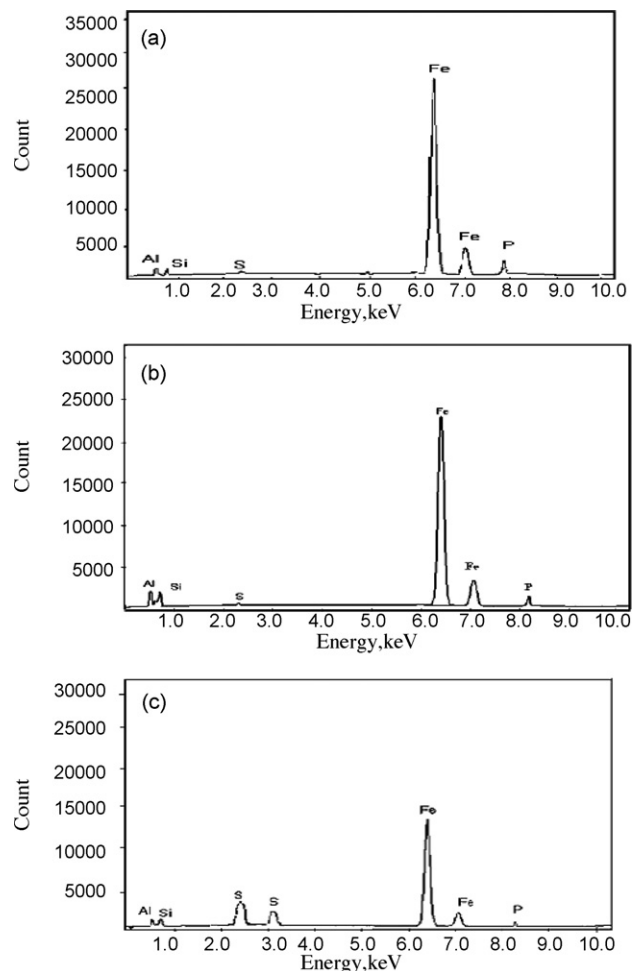


Fig. 9. Energy dispersive X-rays analysis (EDX) of carbon steel samples: (a) polished carbon steel surface, (b) After immersion in 2 M HCl solution for 12 h, (c) After immersion in 2 M HCl solution for 12 h in the presence of 400 ppm of (GT-SH).

from potentiodynamic polarization and EIS techniques are shown in Fig. 8.

3.4. Energy dispersive X-ray analysis (EDX)

The protective film formed on carbon steel surface was analyzed using EDX as shown in Fig. 9. The EDX spectrum of polished car-

bon steel sample in Fig. 9(a) shows a good surface properties, while the spectrum in case of carbon steel sample immersed in 2 M HCl solution without inhibitor molecules (blank) was failed because it is severely weakened by external corrosion as shown in Fig. 9(b). By adding 400 ppm of (GT-SH), the decrease of iron band and appearance of sulfur band was observed due to the formation of a strong protective film of the inhibitor molecules on the surface of carbon steel sample [35] as indicated in Fig. 9(c).

3.5. Scanning electron microscopy (SEM)

The SEM images of the polished carbon steel surface and those immersed in 2 M HCl in the absence and presence of 400 ppm of the inhibitor for 12 h are given in Fig. 10. An image of polished carbon steel surface is shown in Fig. 10(a). The micrograph shows a characteristic inclusion, which is fairly an oxide inclusion [36]. Fig. 10(b) shows an image of carbon steel surface after immersion in 2 M HCl solution. The micrograph reveals that the surface is highly damaged in absence of the inhibitor. Fig. 10(c) shows the image of another carbon steel surface immersed in 2 M HCl solution for the same period in presence of 400 ppm of the inhibitor.

4. Conclusions

The main conclusions of the present study could be summarized in the following points:

1. Thiol derivative of glycolized PET (GT-SH) was synthesized and characterized by FTIR and NMR spectroscopy.
2. (GT-SH) has shown a strong inhibitive effect for the corrosion of carbon steel in 2 M HCl solution during acid cleaning process.
3. Potentiodynamic polarization studies showed that the selected compound suppresses both anodic and cathodic process and thus acts as mixed-type inhibitor but the anodic effect is more pronounced.
4. The results of EIS indicate that the values of C_{dl} tend to decrease and both R_f and η , % tend to increase by increasing the inhibitor concentration.
5. SEM and EDX observations of the electrode surface showed that a film of inhibitor molecules is formed on the electrode surface. This film retarded both the reduction of hydrogen ions (cathodic reaction) and the anodic dissolution of carbon steel (anodic reaction).
6. The high inhibition efficiency (η , %) can be attributed to strong adsorption ability of (GT-SH) molecules on carbon steel surface.
7. Inhibition efficiencies obtained from polarization data are comparable with those obtained from electrochemical impedance spectroscopy measurements and it was found that they are in good agreement.

Acknowledgments

This work has been financially supported by the US-Egypt joint research fund, Washington, DC and Cairo, administrated by the US National Science Foundation.

References

- [1] G. Colomines, J. Robin, G. Tersac, *Polymer* 46 (2005) 3230.
- [2] S. Yao, X. Jiang, L. Zhou, Y. Lv, X. Hu, *Mater. Chem. Phys.* 104 (2007) 301.
- [3] R. Solmaz, G. Kardas, M.C. ulha, B. Yazici, M. Erbil, *Electrochim. Acta* 53 (2008) 5941.
- [4] F. Bentiss, M. Lebrini, M. Lagrenée, M. Traisnel, A. Elfarouk, H. Vezin, *Electrochim. Acta* 52 (2007) 6865.
- [5] M.A. Migahed, A.A. El-Shafei, A.S. Fouda, M.A. Morsi, *Egypt. J. Chem.* 45 (2003) 571.
- [6] M.A. Migahed, *Mater. Chem. Phys.* 93 (2005) 48.
- [7] M.A. Migahed, R.O. Aly, A.M. Al-Sabagh, *Corros. Sci.* 46 (2004) 2503.

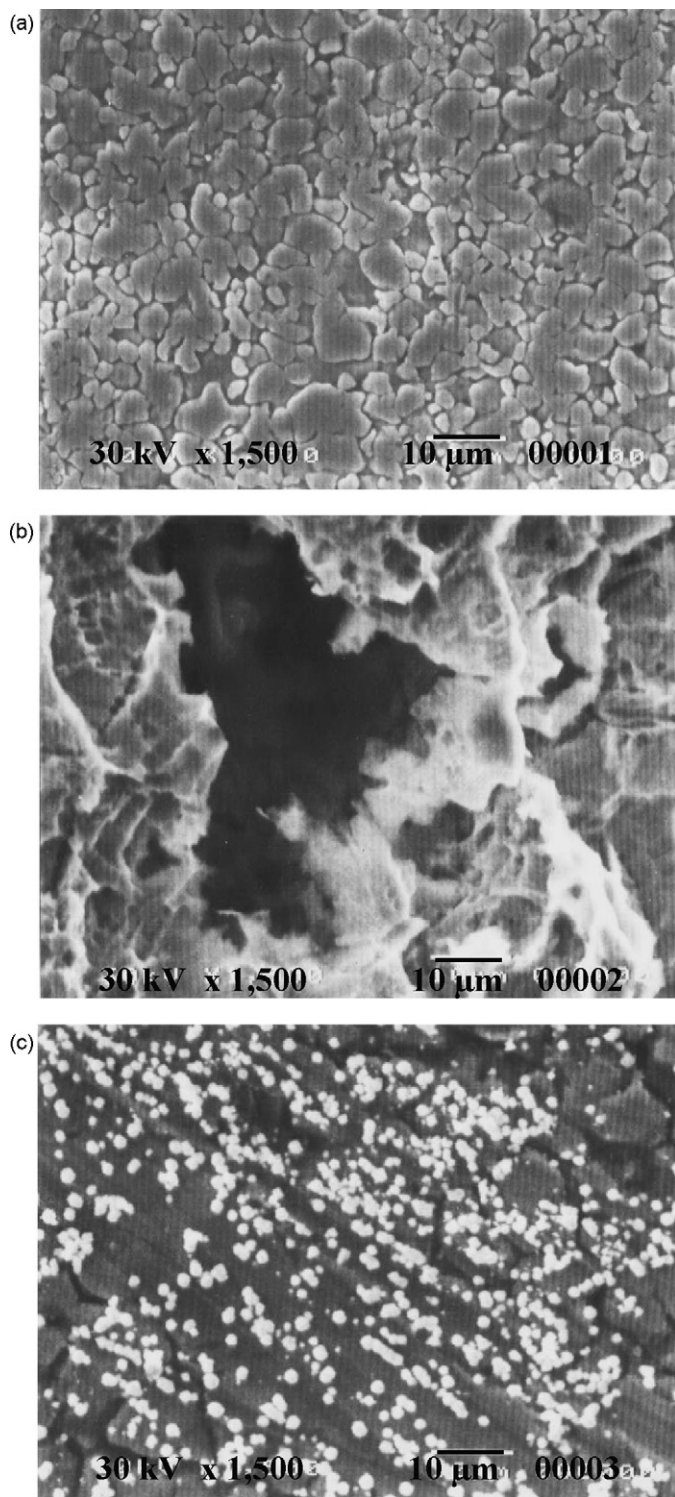


Fig. 10. Micrographs of mild steel surface: (a) after polishing. (b) After immersion in 2 M HCl solution without inhibitor. (c) After immersion in 2 M HCl solution in the presence of 400 ppm of the inhibitor.

- [8] M.A. Migahed, M.A. Abd El-Raouf, A.M. Al-Sabagh, H.M. Abd El-Bary, *Electrochim. Acta* 50 (2005) 4683.
- [9] M.A. Migahed, M.A. Abd El-Raouf, A.M. Al-Sabagh, H.M. Abd El-Bary, *J. Appl. Electrochem.* 36 (2006) 395.
- [10] M.A. Migahed, I.F. Nassar, *Electrochim. Acta* 53 (2008) 2877.
- [11] M.A. Migahed, A.M. Al-Sabagh, N.M. Nasser, Gh.N. Kandile, *J. Disp. Sci. Tech.* 29 (2008) 161.
- [12] M. Tariq Saeed, Sk. Asrof Ali, S.U. Rahman, *Anti-Corros. Meth. Mater.* 50 (2003) 201.
- [13] M. Elachouri, M.S. Hajji, S. Kertit, E.M. Essasi, M. Salem, R. Coundert, *Corros. Sci.* 37 (1995) 381.
- [14] B. Mernari, H. El-Attari, M. Traisnel, F. Bentiss, M. Lagrenee, *Corros. Sci.* 40 (1998) 391.
- [15] G. Schmitt, *Brit. Corros. J.* 19 (1984) 165.
- [16] K.F. Khaled, K. Babic-Samardzija, N. Hackerman, *J. Appl. Electrochem.* 34 (2004) 697.
- [17] K.F. Khaled, *Electrochim. Acta* 48 (2003) 2493.
- [18] L. Tang, X. Li, Q. Qu, G. Mu, G. Lin, *Mater. Chem. Phys.* 94 (2005) 353.
- [19] O.K. Abiola, *Corros. Sci.* 48 (2006) 3078.
- [20] F. Bentiss, F. Gassama, D. Barbry, L. Gengembre, H. Vezin, M. Lagrenee, M. Traisnel, *Appl. Surf. Sci.* 252 (2006) 2684.
- [21] A. Popova, M. Christov, S. Raicheva, E. Sokolova, *Corros. Sci.* 46 (2004) 1333.
- [22] T. Arslan, F. Kandemirli, E.E. Ebenso, I. Love, H. Alemu, *Corros. Sci.* 51 (2009) 35.
- [23] J. Cruz, T. Pangarasu, E. Garcia-choa, *J. Electroanal. Chem.* 583 (2005) 8.
- [24] K. Tameda, J. Nagasawa, F. Nakamishi, K. Abe, *Langmuir* 14 (1988) 3264.
- [25] X. Liu, S. Houyi Ma, G. Liu, L. Shen, *Appl. Surf. Sci.* 235 (2006) 814.
- [26] J.M. West, *Electrodeposition and Corrosion Process*, second ed., Van Nostrand Reinhold, London, 1970, p. 93.
- [27] C.E. Kaan, H. Mustafa, *Corros. Sci.* 48 (2006) 797.
- [28] H.P. Lee, K. Nobe, *J. Electrochem. Soc.* 133 (1986) 2035.
- [29] S.S. Abd El-Rehim, H.H. Hassan, M.A. Amin, *Corros. Sci.* 46 (2004) 5.
- [30] F. Mansfeld, M.W. Kending, S. Tsai, *Corrosion* 37 (1981) 301.
- [31] A.P. Yadav, A. Nishikata, T. Tsuru, *Corros. Sci.* 46 (2004) 169.
- [32] A. Galal, N.F. Atta, M.H.S. Al-Hassan, *Mater. Chem. Phys.* 89 (2005) 38.
- [33] M.A. Ajmal, J. Rawat, M.A. Quarishi, *Bri. Corros. J.* 24 (1999) 220.
- [34] K.F. Khaled, *Appl. Surf. Sci.* 252 (2006) 4120.
- [35] M.A. Amin, *J. Appl. Electrochem.* 36 (2006) 215.
- [36] ASTM 45-87, *Annual Book of ASTM Standard*, vol. 11, ASTM, Philadelphia, PA, 1980, p. 125.